Non-Destructive Surface Roughness Analysis for Polymer-Based Products: Integrating Laser Speckle Contrast and Stylus Profilometry

Dr Adam Jones
Faculty of Computing, Engineering and Science
University of South Wales
United Kingdom
adam.jones@southwales.ac.uk

Dr Samuel Eurfyl Davies
Faculty of Computing, Engineering and Science
University of South Wales
United Kingdom
eurfyl.davies@southwales.ac.uk

Dr Kang Li
Faculty of Computing, Engineering and Science
University of South Wales
United Kingdom
kang.li@southwales.ac.uk

This study introduces a novel approach for measuring surface roughness in polymer-based samples using laser speckle photometry principles, offering potential for non-contact and non-destructive in-process measurements. A methodology for characterising surface roughness offline for polymer samples is outlined, utilising stylus profilometry, a technique not commonly employed in polymer manufacturing. Investigations into the reliability and stability of laser speckle on polymer-based products with various shape profiles were conducted, resulting in successful outcomes through mean intensity matching techniques. This enabled the correlation of surface roughness with two laser speckle statistical parameters: laser speckle contrast and binary digitization techniques. This research provides valuable insights for advancing surface roughness measurement techniques in polymer manufacturing processes.

Keywords: Surface roughness, Polymers, Laser speckle, MATLAB, Stylus Profilometry, Non-Destructive Testing

I. Introduction

Surface roughness at the nano-micro scale presents a common challenge in manufacturing, impacting product quality and performance. This challenge is evident in various industries, including polymer extrusion line production, where even minor surface irregularities could affect functionality. Current measurement solutions involve tactile testing, which is time-consuming and inconsistent. This research aimed to explore cost-effective, in-process techniques for evaluating surface roughness, focusing on non-contact, non-destructive methods with high-speed measurement capabilities. By addressing this challenge, this research sought to enhance manufacturing efficiency and product quality across polymer manufacturing industries. The main parameters for this research were referenced to the varying product characteristics at the industrial partner, including colour, shape, and diameter of samples under test. In this particular extrusion process, polymers are produced in three shapes: round, gear, and petal profiles, each controlled by specific die sets featuring macroscopic surface features on both the gear and petal profiles. Previously, surface roughness was measured in-line and offline by operator touch (tactile feedback), with no available system capable of performing these measurements consistently in both modes. The smallest sample diameter was quantified as 600 µm and additionally, the colour variation of the extruded polymers was also investigated, indicating several challenges in the development of an in-process evaluation technique.

II. Background Research

Surface roughness is the measurable quality of an object's texture, determined by the vertical differences in its surface compared to an ideal form (based on the design specifications of the object being manufactured, representing the theoretical perfect surface). These differences can range from significant variations, indicating high roughness, to minimal differences, indicating low roughness.. This characteristic is vital in defining an object's specifications as it directly affects its interaction with the surrounding environment. The two most common parameters used to measure surface roughness are illustrated in Fig 1 [1], R_a and R_q. The arithmetic average (R_a) of the roughness profile (typically measured in µm) is calculated as the absolute values of the height deviations from the nominal surface z(x), which represents the average roughness height over the evaluation length L. The root mean square (R_q) provides a measure of the root mean square average of the profile heights z(x) over the evaluation length L (also measured in µm).

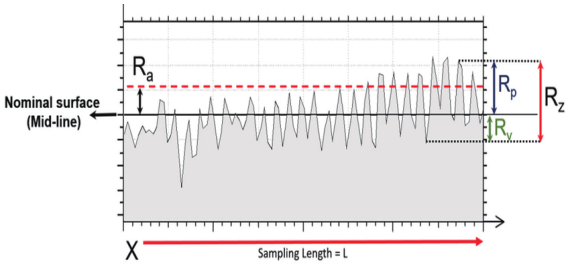

Fig 1. Surface roughness visualisation [1]

The mathematical descriptions for R_a and R_q are provided by (1) and (2) below, where L represents the length of the measurement test, and z(x) indicates the surface height deflection in reference to the measured nominal surface value.

$$R_a = \frac{1}{L}\int_0^L z(x)dx \tag{1}$$

$$R_q = \sqrt{\frac{1}{L}\int_0^L z^2(x)dx} \tag{2}$$

A. Review of surface roughness analysis techniques

There are several methods available for quantifying surface roughness, including White Light Interferometry (WLI) [2], Atomic Force Microscopy (AFM) [3], stylus profilometry [4-9], Chromatic Confocal Microscopy (CCM) [10], and Scanning Electron Microscopy (SEM) [11]. Typically, mechanical stylus profilometry instruments are employed for surface roughness measurement, however, this approach necessitates physical contact with the sample and is impractical for continuous production settings [12]. Some studies propose optical techniques as an alternative, offering advantages such as low cost, non-contact, non-destructive

measurement, and high-speed capabilities. One such technique utilises Laser Speckle Photometry (LSP) principles [4-6, 8, 9, 12-14]. Although various experimental setups and regression techniques have been proposed to relate surface roughness to laser speckle parameters, no studies have yet applied this technique to polymer-based samples with cylindrical profiles, various colours, varying sample thicknesses, and varying shape profiles. This research aimed to bridge this gap by applying laser speckle photometry principles for these industrial settings for potential in-process surface roughness quantification.

B. Laser speckle

Laser speckle is a pattern observable when a highly coherent light source undergoes diffuse reflection upon encountering a surface with a rough texture. This phenomenon arises from the intricate interaction of various reflected wave fronts, leading to fluctuations in intensity as these waveforms interfere. Initially regarded as a limitation of laser technology, laser speckle has since emerged as a prevalent technique in optical sciences, notably for the precise measurement of surface roughness. Fig 2. below illustrates a typical laser speckle pattern observed at the interface of a rough surface. Manifesting as a granular structure, the bright regions signify constructive interference, while the darker regions signify destructive interference. Notably, the image also portrays saturation effects, where the granular patterns become saturated because of the detector's intensity limit. In the context of surface roughness assessment, the accurate capture and analysis of interference effects are paramount for establishing robust calibration parameters. This ongoing investigation endeavors to develop methodologies aimed at mitigating saturation effects in captured images, thereby enhancing the accuracy and reliability of surface roughness measurements.

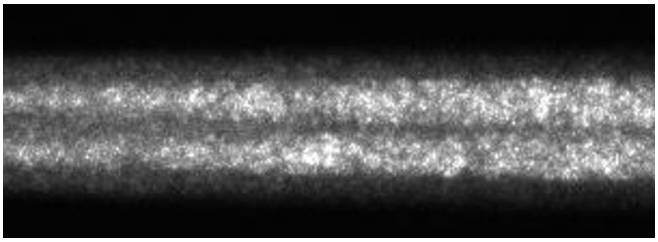

Fig 2. Laser speckle pattern on polymer-based cylindrical samples

C. Laser speckle statistical parameters

Following the capture of a laser speckle pattern image, the subsequent step involves assessing surface roughness through various regression parameters. While many of these techniques have been delineated in the literature, primarily for metallic surfaces, this article offers a concise overview of each parameter for evaluation.

a) Mean intensity: Mean intensity (MI) represents the average brightness of an image, determined by summing the intensities of all pixels within a region of interest (ROI) and dividing by the total pixel count in that region. Xu et al. [9] conducted experimental research exploring various laser speckle photometry parameters to determine correlation among metallic samples exhibiting diverse surface roughness. One parameter under scrutiny was the effect on MI across a specified region of interest within the captured speckle image. Their findings unveiled a non-linear correlation between surface roughness and MI, suggesting that light scattered from rough surfaces disperses more than from smoother ones, resulting in heightened intensity with increased surface roughness. Equation (3) below defines the calculation of MI within a defined region of interest, where N signifies the total pixel count, and I_i represents the intensity at each pixel *i*.

$$\bar{I} = \frac{1}{N}\sum_{i=1}^{N} I_i \tag{3}$$

b) Standard deviation: Standard deviation (SD) serves as a measure of the spread of intensity values within an image region of interest relative to its mean intensity. A low SD indicates that pixel intensities are tightly clustered around the mean intensity, while a high SD suggests significant deviation from the mean, signifying a wide range of intensity values across the camera sensor. Jeyapoovan et al. [4] identified a linear relationship between variance (the square of SD) and surface roughness for milled and ground metallic samples. Equation (4) below defines the calculation of SD in reference to the total pixel count (N), mean intensity and intensity at each pixel.

$$\sigma = \sqrt{\frac{\sum_{i=1}^{N}(I_i - \bar{I})^2}{N}} \tag{4}$$

c) Speckle contrast: The speckle contrast of an image is determined by dividing the standard deviation of a region of interest by its mean intensity value. Xu et al. [9] employed this parameter to investigate the surface roughness of their samples, observing that higher surface roughness led to a notable reduction in speckle contrast. Mathematically, contrast (K) can be expressed as the ratio of the standard deviation (σ) to the mean intensity I of the entire pixel area.

$$K = \sigma \,/\, \bar{I} \tag{5}$$

d) Binary digitization: The process of binary speckle digitization involves multiple steps: starting with capturing the speckle pattern image, followed by isolating a designated region of interest within the image. Subsequently, a binary transformation is applied to the image using a predetermined threshold value, which assigns each pixel a value of either 0 or 1 based on this threshold. Finally, the ratio of white pixels to dark pixels is analysed to establish a correlation with actual surface roughness. This method has been widely used in evaluating surface roughness of steel samples across various studies [5, 9, 12, 13], indicating its potential as a practical tool for in-situ surface roughness measurement, especially for dynamic surfaces.

III. METHODOLOGY

The experimental phase of this research involved the collection and preparation of Polyurethane (PU) samples from the industrial partner, analysing samples using microscopy to evaluate sample profiles, characterise surface roughness using stylus profilometry, setting up the experimental hardware for laser speckle analysis, and acquiring and processing speckle images. Statistical analysis of the speckle images was conducted to establish correlation between target surface roughness (using profilometry results) against laser speckle contrast and binary digitisation parameters.

A. *Sample specifications*

Multiple samples were gathered for experimental investigation, encompassing operator quality feedback for three conditions: "Pass," "Fail," and "Borderline Pass." Each shape profile, including Round, Gear, and Petal shapes, was represented in the samples, with various colours provided exclusively for the round shape. The samples exhibited a range of diameters and were measured using a Micrometer to establish a correlation with image processing pixel area for laser speckle analysis. The smallest sample diameter provided by the industrial partner was 0.6 mm, which was used to direct the ROI on each speckle image.

B. *Microscopy analysis*

Microscopic analysis was carried out using an Infinity Kohler Trinocular Compound Microscope with a magnification of 40x to assess the various shape profiles of the samples. The findings of this investigation are depicted in Fig 3. showcasing the round and petal profiles. In the round shape profiles, no macroscopic surface features are evident, whilst conversely the petal shape profile displays sharp macroscopic surface features at periodic intervals around the product circumference resultant from the die-set used in the extrusion process.

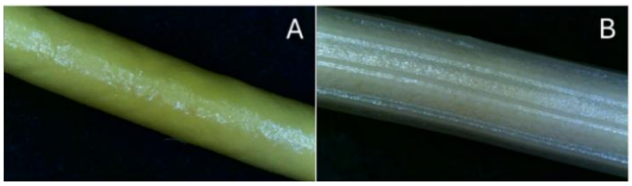

Fig 3. Sample microscopy analysis. Illustration of round profile (A) and illustration of petal profile (B)

C. *Stylus profilometry analysis*

Two sets of samples were provided for analysis. The first set aimed to examine shape profiles, comprising nine samples: three for each shape category, namely "Pass," "Borderline Pass," and "Fail." The second set focused on investigating the impact of colour. It included nine round-shaped samples, featuring various colours and a wider range of surface roughness. Each sample was approximately 150 mm in length and clearly labelled. The thinnest end of each sample was selected for measurement, aligning with the aim of laser speckle capture experiments, which targeted products as thin as 0.6 mm. The thickness of each sample was meticulously measured using a digital micrometer, ensuring accuracy at the micron level. Surface roughness was assessed using a stylus profilometry instrument (Mitutoyo Surftest SJ-210).

Fig 4. Mitutoyo Surftest SJ-210 with 3.00 µm Ra calibration reference

Adjustments to the instrument parameters were necessary to enable precise measurement of the cylindrical shape profiles. A specific procedure was devised to secure the samples for measurement, with the optimal method found to be affixing them to a custom developed assembly stand. Occasionally, the instrument failed to capture a measurement, typically when the stylus probe lost contact with the sample, resulting in no data recorded. To address this issue, the measurement speed was increased to 0.75 mm/s, and the number of sampling lengths was reduced from 5 to 2. Calibration of the instrument was verified using a metallic reference sample with a known surface roughness of 3.00 µm R_a, yielding a measurement of 3.050 µm R_a, within tolerance. Three measurements were taken for each sample, and the average was calculated to assess potential variations in surface roughness across different areas. These areas were demarcated with tape for further experimentation. Longitudinal measurements were conducted to minimise any surface roughness resulting from the shape of the product. The parameters of the Mitutoyo Surftest SJ-210 were adjusted to ensure accurate surface roughness measurements for the cylindrical samples. These parameters are outlined in Table I.

TABLE I. Mitutoyo Surftest SJ-210 parameters

Measurement type	Roughness
Calibration standard	ISO 1997
Filter	Gaussian
Measurement speed	0.75 mm / s
λc	2.5 mm
λs	8 µm
N	2
Range	Auto

Two sets of sample batches were examined, revealing varying surface roughness across different measurement points. The initial sample batch aimed to characterise surface roughness in relation to operator feedback conditions, including pass, borderline pass, and failed product scenarios. These findings were subsequently utilised for laser speckle analysis. Notably, distinct differences were observed between operator-defined pass and fail scenarios, directly correlating with the measured surface roughness. The profilometry results for the first sample batch are defined in Table II.

TABLE II. Batch 1 profilometry results

Profile	**Tactile analysis**	**Profilometry (µm RA)**
Round	Pass	0.99
Round	Borderline pass	1
Round	Fail	2.85
Gear	Pass	0.95
Gear	Borderline pass	1.05
Gear	Fail	3.21
Petal	Pass	1.2
Petal	Borderline pass	1.55
Petal	Fail	2.9

For samples categorised as pass conditions by operators, the surface roughness was consistently low across all three shapes, measuring less than 1.30 µm R_a. Samples designated as borderline pass exhibited slightly higher surface roughness compared to pass conditions for round and gear profiles, with significantly higher surface roughness observed for petal profiles. Surface roughness for all shapes categorised as borderline pass was less than 1.90 µm R_a. In contrast, samples

categorised as fail conditions by operators displayed higher surface roughness across all shapes, exceeding 2.30 µm R_a. Based on these results, a roughness threshold for failure state was quantified for greater than 1.90 µm R_a. The second sample batch comprised entirely of round-shaped profiles were procured to explore the effects of product colour and to introduce a wider range of surface roughness variations. Operator feedback conditions were not provided for this batch. However, upon tactile examination of the samples and the results obtained from batch 1, it became evident which samples had the lowest and highest surface roughness, which also supported the notion of a 1.90 µm R_a surface roughness threshold for a failure state. The profilometry results for the second sample batch are defined in Table III. It is crucial to emphasize that different colours can correspond to different surface roughness levels. Therefore, it was essential to devise a method that specifically isolated the colour variable for analysis.

TABLE III. Batch 2 profilometry results

Colour	Profilometry (µm RA)
Purple	0.81
Orange	0.93
Yellow	0.94
Green	1.57
Light green	1.65
Yellow	1.78
White	1.79
Brown	1.93
Green	2.08

D. Laser speckle experimental setup

The laser speckle experimental setup was adjusted to investigate the reliability of capturing laser speckle patterns on polymer-based cylindrical products, an area with limited literature. Challenges included the products' variable diameters, with the smallest measuring 0.6 mm. To address this, a standardised region of interest measuring 100 x 20 pixels was selected for all samples, based on the specifications of the Thorlabs CS135MUN camera and its optics (5 – 50 mm variable focus lens). The samples were available in three shapes: round, gear, and petal, posing complexities in characterising surface roughness across different shapes. To account for this, a larger region of interest was chosen longitudinally to the sample profile within the 100 x 20-pixel area. Additionally, separate mathematical models for speckle regression were developed for each shape to ensure measurement accuracy. Moreover, the products featured various colours, impacting light sensitivity, and introducing saturation effects in laser speckle patterns. Although increased surface roughness was expected to lead to higher light scattering, excessive saturation degraded regression quality. To mitigate these effects, different lasing wavelengths within the visual and infrared spectrum were explored using Thorlabs CPS405, CPS520, CPS635, and CPS980 laser diode modules. Despite considering variable power laser diodes, implementing mean intensity control via camera exposure time proved more effective in addressing saturation and colour issues. The experimental setup (depicted in Fig 5) comprised of a laser source (1), FW2AND neutral density filter wheel from Thorlabs (2), ED1-C20-MD circular diffuser from Thorlabs (3), sample stage with tension control (4), and the camera and optics system (5). The neutral density filter wheel was included to assess whether saturation and colour effects could be mitigated but was deemed inefficient due to unnecessary mechanical movement in the optical setup. The circular diffuser was necessary to provide top-hat illumination at the sample surface, evenly spreading coherent light from the laser diode. Various geometrical parameters were investigated, including the laser diode's angle of incidence, distance from the laser source to diffuser, diffuser-to-sample distance, and sample-to-camera system distance. Optimum parameters for this application included a low angle of incidence (18 degrees), 45 mm distance from the laser source to the engineered diffuser, 100 mm distance from the diffuser to the sample surface, and 30 mm distance from the sample surface to the camera system. However, maintaining a near-normal lasing incident angle minimised variations in component distances to the sample stage when implementing mean intensity control using camera exposure time.

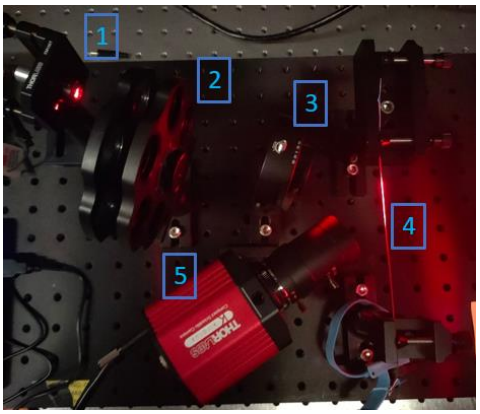

Fig 5. Experimental setup for laser speckle capture

E. Image aquisition

The CS135MUN camera's ThorCam software was employed to capture images of the samples. Initially, the sample under examination was mounted on the tension control mount and illuminated with white light to confirm focus alignment with the system. The laser source was activated, and live image capture via ThorCam software was monitored for any saturation effects and to verify the central alignment of the sample within the image sensor. To aid in aligning the sample to the centre, a reticule tool within the software was utilised, as depicted in Figure 6.

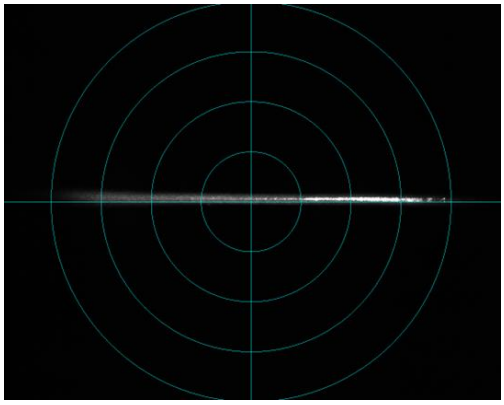

Fig 6. ThorCam reticule for sample alignment

During this phase, a region of interest corresponding to the smallest sample diameter size (0.6 mm) was selected,

resulting in a 100 x 20-pixel area for analysis, equivalent to 2000 pixels. The histogram tool within the software was utilised to assess the mean intensity across the selected pixel range, ensuring a consistent mean intensity value of 550 (representing a 10-bit analog-to-digital converter in the camera sensor) was maintained for all samples. This mean intensity matching technique facilitated the isolation of pixel area intensity for each sample, enabling investigation into standard deviation, contrast, and binary digitization, irrespective of sample colour, potential in-process effects, and saturation issues. Adjusting the exposure time of the camera proved to be the most effective method for controlling the mean intensity value across the pixel range. Images for each sample were then saved for subsequent image processing, with mean, standard deviation, and contrast values recorded from the ThorCam software for each sample.

IV. RESULTS & DISCUSSION

A. *Offline charactertisation*

Before this study, the industrial partner lacked a technique for measuring the surface roughness of their products. This research has introduced a procedure utilising stylus profilometry to assess surface roughness offline, enabling further exploration of applicable in-process measurement techniques. The results revealed a concordance between surface roughness assessed via stylus profilometry and operator tactile feedback for pass and fail conditions. However, subjective interpretations were observed in the transitional regions between these states, influenced by operator variability in quality assessments. Notably, the characterised surface roughness did not exhibit significant distinctions between pass and borderline pass conditions.

B. *Reliability of laser speckle detection*

The implementation of neutral density filters proved ineffective, as they uniformly attenuated the laser source regardless of sample parameters. Although variable power lasers were effective, they introduced complexity to the hardware setup. However, controlling the camera's exposure time proved highly effective and could be achieved using simple control logic, with mean intensity as the setpoint value and exposure time as the control variable. Nevertheless, the primary challenge throughout the investigation was aligning each captured image with various characteristics. By standardising the mean intensity of the pixel area, regardless of colour, the mean intensity variable could be isolated, facilitating the calculation of a normalised laser speckle contrast result. Based on these developed principles, it was determined that laser speckle patterns could be reliably captured on the polymer products, paving the way for further research into correlating statistical parameters of laser speckle with the actual surface roughness of the provided samples.

C. *Laser speckle contrast analysis*

The laser speckle contrast analysis was conducted according to the methodology outlined, with a lasing wavelength of 980 nm and an optical power of 5 mW providing the optimal results in terms of correlating speckle contrast to surface roughness. Additionally, employing a low angle of incidence for the laser source (less than 20 degrees from normal to the sample surface) provided optimal imaging conditions with minimal saturation across the measurement area. The results, illustrated in Fig 7, show a positive linear trend between contrast and surface roughness for the round shape, while the gear and petal shapes exhibited negative trends. Given the macroscopic features present on the surface of gear and petal profiles, these results were expected to differ from those of round shape profiles due to principles of light scattering at the surface roughness interface. The first sample set, characterised by minimal variation in surface roughness and colour, prompted the acquisition of a second sample set for analysis. This set, comprising nine samples all round shape, exhibited greater variation in colour and surface roughness. The results mirrored those of the first sample set, showing a linear increase in contrast as surface roughness increased. The implementation of mean intensity matching effectively mitigated saturation effects and variations in sample colour, indicating that laser speckle contrast could predict surface roughness for round shape samples, however more sample variability is required for the gear and petal shape product profiles before feasibility assessment is made and subsequent in-process trials.

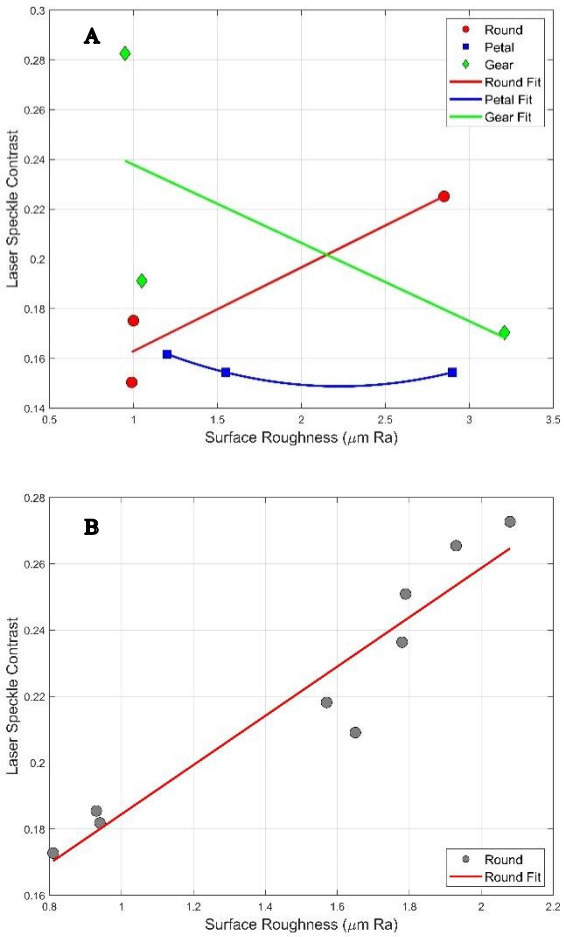

Fig 7. Laser speckle contrast for sample batches 1 (**A**) and 2 (**B**)

D. *Binary digitisation analysis*

To establish the relationship between White/Black (W/B) ratio and profilometry surface roughness results, a bespoke MATLAB application was developed. This application facilitated the retrieval of stored images from the ThorCam trials, generation of the region of interest based on the 100 x

20-pixel area, and execution of binary transformation using Otsu's thresholding method. The calculation of the white to black ratio involved determining the binary levels of 0 (black) and 255 (white) pixels on the transformed image and dividing them to yield the numerical result. As illustrated in Fig 8. the W/B ratio trendlines closely mirrored the laser speckle contrast results.

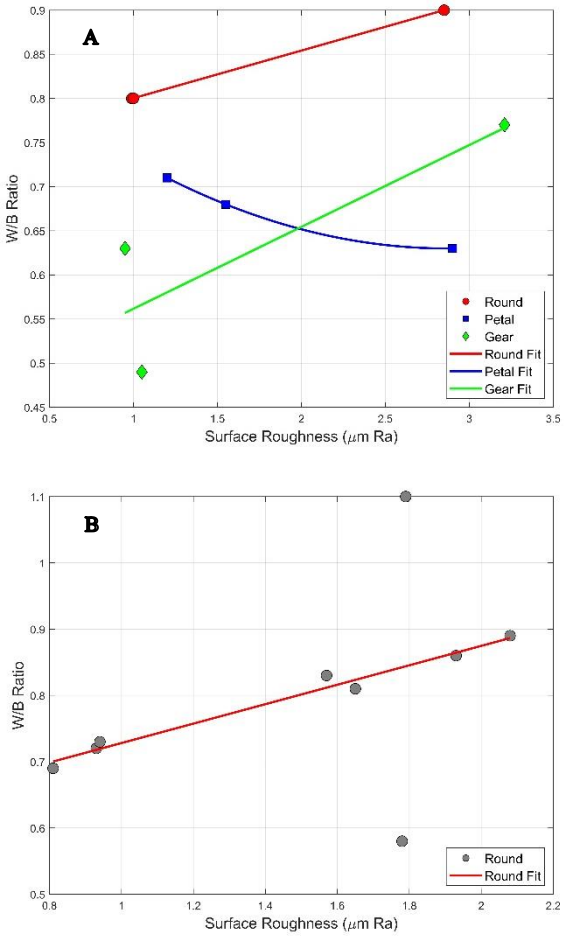

Fig 8. W/B ratio for sample batches 1 (**A**) and 2 (**B**)

V. Conclusion

In summary, the devised method for offline surface roughness assessment of polymer-based cylindrical products using a Mitutoyo Surftest SJ-210 stylus profilometer proved effective, distinguishing clear pass and fail conditions through surface roughness characterisation and comparison with operator tactile feedback. Despite encountering challenges such as variations in sample colour, diameter, and shape profile, surface roughness analysis via laser speckle contrast yields promising innovation. Currently, this system has undergone further development and integration into a live production environment, yielding further positive outcomes for the round shape profile. Future research endeavours aim to leverage the data generated from this setup to enable non-contact, non-destructive, and high-speed evaluation of surface roughness not only for polymer-based products but also for a diverse range of samples.

Acknowledgments

The authors of this study wish to extend their heartfelt appreciation to our industrial collaborators in polymer extrusion and systems integration and automation for their unwavering commitment and contributions to the project's progress. Additionally, we would like to express our gratitude for the financial support provided by the SMART CYMRU grants, which have been instrumental in facilitating this project's continuing advancement.

References

[1] N. Tekçe, S. Fidan, S. Tuncer, D. Kara, and M. Demirci, "The effect of glazing and aging on the surface properties of CAD/CAM resin blocks," The journal of advanced prosthodontics, vol. 10, no. 1, pp. 50-57, 2018.

[2] S. Adi, H. Adi, H.-K. Chan, P. M. Young, D. Traini, R. Yang, and A. Yu, "Scanning white-light interferometry as a novel technique to quantify the surface roughness of micron-sized particles for inhalation," Langmuir, vol. 24, no. 19, pp. 11307-11312, 2008.

[3] R. De Oliveira, D. Albuquerque, T. Cruz, F. Yamaji, and F. Leite, "Measurement of the nanoscale roughness by atomic force microscopy: basic principles and applications," Atomic force microscopy-imaging, measuring and manipulating surfaces at the atomic scale, 2012, vol. 3.

[4] T. Jeyapoovan, M. Murugan, and B. C. Bovas, "Statistical analysis of surface roughness measurements using laser speckle images," in Statistical analysis of surface roughness measurements using laser speckle images. IEEE, 2012, pp. 378-382.

[5] E. Kayahan, H. Oktem, F. Hacizade, H. Nasibov, and O. Gundogdu, "Measurement of surface roughness of metals using binary speckle image analysis," Tribology International, vol. 43, no. 1-2, pp. 307-311, 2010.

[6] M. Nicklawy, A. Hassan, M. Bahrawi, N. Farid, and A. M. Sanjid, "Characterizing surface roughness by speckle pattern analysis," 2009.

[7] K. Saliou, F. Hilt, G. Fischer, T. Hildebrandt, P.-P. Grand, and E. Drahi, "Powerful topographic analyzing method using fast Fourier transform for c-Si solar cells and advanced technologies," in Powerful topographic analyzing method using fast Fourier transform for c-Si solar cells and advanced technologies. AIP Publishing LLC, 2019, pp. 020013.

[8] S. Toh, H. Shang, and C. Tay, "Surface-roughness study using laser speckle method," Optics and Lasers in Engineering, vol. 29, no. 2-3, pp. 217-225, 1998.

[9] D. Xu, Q. Yang, F. Dong, and S. Krishnaswamy, "Evaluation of surface roughness of a machined metal surface based on laser speckle pattern," The Journal of Engineering, vol. 2018, no. 9, pp. 773-778.

[10] S. Fu, W. S. Kor, F. Cheng, and L. K. Seah, "In-situ measurement of surface roughness using chromatic confocal sensor," Procedia CIRP, vol. 94, pp. 780-784, 2020.

[11] A. Kakaboura, M. Fragouli, C. Rahiotis, and N. Silikas, "Evaluation of surface characteristics of dental composites using profilometry, scanning electron, atomic force microscopy and gloss-meter," Journal of Materials Science: Materials in Medicine, vol. 18, no. 1, pp. 155-163, 2007.

[12] D. R. Patel and M. Kiran, "Non-contact surface roughness measurement using laser speckle technique," in Non-contact surface roughness measurement using laser speckle technique. IOP Publishing, 2020, pp. 012007.

[13] A. Hamed, H. El-Ghandoor, F. El-Diasty, and M. Saudy, "Analysis of speckle images to assess surface roughness," Optics & Laser Technology, vol. 36, no. 3, pp. 249-253, 2004.

[14] N. Mashiwa, T. Furushima, and K. Manabe, "Novel non-contact evaluation of strain distribution using digital image correlation with laser speckle pattern of low carbon steel sheet," Procedia Engineering, vol. 184, pp. 16-21, 2017.